used immunoprecipitation and immunoblotting to show that the antibodies to the COOH-terminal peptide from Cdc2 recognized Cdc2 but not Cdk2, and conversely that the antibodies to the COOH-terminal peptide from Cdk2 recognized Cdk2, but not Cdc2 (A.K. and J.M.R., unpublished observations).
12. A. Giordano *et al.*, *Cell* **58**, 981 (1989).
13. A. Giordano *et al.*, *Science* **253**, 1271 (1991).
14. Essentially the same profile of cyclin E–associated proteins was observed by two-dimensional PAGE of immunoprecipitates from ^{35}S-labeled extracts of MANCA cells (B. Robert Franza, Antonio Giordano, Andrew Koff, James M. Roberts, unpublished data).
15. Spots a and b were also seen in longer exposures of immunoprecipitates from [^{35}S]methionine-labeled extracts.
16. Anti–cyclin E immunoprecipitates from MANCA and HeLa cells also contained a 45-kD protein that was detected in immunoblots with affinity-purified anti–cyclin E, and this protein precisely comigrated on PAGE with in vitro–translated cyclin E (A.K. and J.M.R., unpublished observations).
17. Immunoblots of anti–cyclin E immunoprecipitates with the anti–cyclin E detected a single protein at 45 kD. Therefore, the other proteins found in anti–cyclin E immunoprecipitates—phosphoprotein x and spot 3—were most likely bound to cyclin E and not simply detected because of cross-reactivity with this antibody.
18. A similar spot has not been observed in two-dimensional PAGE of proteins that bind the peptide p13 nor has it been seen in immunoprecipitates with G8 antiserum, which recognizes many members of the Cdc2 protein family (*13*). We have not observed a phosphoprotein of similar molecular size in immunoprecipitates with an antiserum to the conserved PSTAIRE domain of the Cdc2 protein family.
19. The identification of Cdk2 in cyclin E immunoprecipitates has been confirmed with three different antisera independently raised against peptides corresponding to the COOH-terminal portion of human Cdk2. All three antisera recognize Cdk2 but not Cdc2 (*10, 11, 20*).
20. S. Elledge *et al.*, *Proc. Natl. Acad. Sci. U.S.A.* **89**, 2907 (1992).
21. Immunodepletion of Cdc2 protein from MANCA cell extracts had no effect on the amount of cyclin E–associated kinase whereas depletion of Cdk2 protein removed 50 to 80% of the cyclin E–associated kinase (A.K. and J.M.R., unpublished observations).
22. When these proteins were overexpressed in insect cells infected with baculovirus vectors, their intracellular concentrations were approximately 5 to 10 μM. To study the binding of cyclin E to Cdc2 and Cdk2, we diluted the extracts so that the concentration of these proteins was closer to normal physiologic levels, 0.2 μM.
23. The absolute amounts of kinase activity detected in these experiments did not correlate with the abundance of the particular cyclin-Cdk complexes and was probably limited by the abundance of a kinase that activates Cdk (*27*). Therefore an estimation of the specific activities of these particular complexes is not yet possible.
24. F. Girard, U. Strausfeld, A. Fernandez, N. Lamb, *Cell* **67**, 1169 (1991).
25. M. Ohtsubo and J.M.R., in preparation.
26. For H1 kinase assays, 8.3×10^6 cells were sonicated in 100 μl of H1 lysis buffer [50 mM tris (pH 7.4), 0.25 M NaCl, 0.5% Nonidet P-40 containing the following protease inhibitors: 1 mM phenylmethylsulfonyl fluoride (PMSF), 20 μg/ml *N*-thosylphenylalanine chloromethyl ketone (TPCK), 20 μg/ml soybean trypsin inhibitor, 10 μg/ml leupeptin]. Lysates were centrifuged at 13,000*g* for 10 min at 4°C and the supernatant was diluted with an equal volume of H1 lysis buffer. Extract (50 μl) was subjected to immunoprecipitation with anti–cyclin E (2 μl) or anti-Cdc2 (2 μl) for 1 hour, or with the C160 monoclonal antibody (5 μl) for 30 min. Rabbit antibodies to mouse immunoglobulin G (2 μl) were added and the mixture was incubated for 30 min. Immune complexes were collected on protein A Sepharose (Pierce) and then washed twice with lysis buffer and four times with H1 kinase buffer [20 mM tris (pH 7.4), 7.5 mM $MgCl_2$, 1 mM DTT]. Kinase reactions were performed as described (*3*).
27. D. Desai, Y. Gu, D. Morgan, *Molec. Biol. Cell* **3**, 571 (1992).
28. The QUEST regulatory protein quantitative database coordinates for two-dimensional gel-resolved spots in this report are: cyclin E isoforms: 1, HH11; 2, HH21; and 3, GH11. Cyclin E–associated protein: *x*, EE11; and Cdk2 isoforms: 1, RE41; 2, QE21; 3, NE11; a, TE31; b, TE41; c, RE51; and d, QE31. J. I. Garrels and B. R. Franza, *J. Biol. Chem.* **264**, 5823 (1989).
29. We thank R. Marraccino and M. Ohtsubo for help and advice during the course of this work. We also thank K. Keegan and S. Halegoua for contributing to our analysis of PC12 cell differentiation, and J. Schumacher, K. Carlson and R. Richman for help preparing antisera. A.G. and R.F. acknowledge support from the Freeman Charitable Trust and from James Watson. A.G. was supported by a fellowship from the Irvington Foundation. *QUEST* 2D gel facility and P. Renna and J. Duffy are thanked for performing the two-dimensional gels and preparing the photography and artwork, respectively. D.M. was supported by a Searle Scholars Award from the Chicago community trust and by a grant from the NIH. K.Y. and T.N. were supported by Grants-in-aid for Scientific Research and for Cancer Research from the Ministry of Education, Science and Culture and the Science and Technology Agency of Japan. S.E. is a PEW scholar in the biomedical sciences and this work was supported in part by a grant from the NIH to S.E. J.W.H. is the recipient of an American Cancer Society Junior Faculty Award. A.K. was supported by a virology training grant from the NIH. J.R. is a Lucille P. Markey scholar in the biomedical sciences. This work was supported in part by grants from the NIH and from the Lucille P. Markey Charitable Trust.

4 June 1992; accepted 16 July 1992

Trypsin-Sensitive, Rapid Inactivation of a Calcium-Activated Potassium Channel

Christopher R. Solaro and Christopher J. Lingle*

Most calcium-activated potassium channels couple changes in intracellular calcium to membrane excitability by conducting a current with a probability that depends directly on submembrane calcium concentration. In rat adrenal chromaffin cells, however, a large conductance, voltage- and calcium-activated potassium channel (BK) undergoes rapid inactivation, suggesting that this channel has a physiological role different than that of other BK channels. The inactivation of the BK channel, like that of the voltage-gated Shaker B potassium channel, is removed by trypsin digestion and channels are blocked by the Shaker B amino-terminal inactivating domain. Thus, this BK channel shares functional and possibly structural homologies with other inactivating voltage-gated potassium channels.

Calcium-activated K^+ channels provide a link between elevations of cytosolic Ca^{2+} and membrane excitability (*1*). The physiological functions of different types of Ca^{2+}-activated K^+ channels are thought to reflect intrinsic differences in kinetics of activation, voltage dependence, and Ca^{2+} sensitivity (*2*). However, at a given membrane potential, Ca^{2+}-activated K^+ channels are, in general, thought to function as persistent sensors of the submembrane Ca^{2+} concentration (*2, 3*). Here, we report that a large conductance, voltage- and Ca^{2+}-activated K^+ channel, often termed the BK channel (*4*), can undergo rapid and virtually complete inactivation, suggesting a new physiological role for this channel distinct from that of noninactivating BK channels (*5*). Although the relation between BK channels and the family of voltage-gated K^+ channels is not known, BK channel inactivation and inactivation of some voltage-gated K^+ channels (*6–8*) share a number of striking similarities.

Department of Anesthesiology, Washington University School of Medicine, St. Louis, MO 63110.

*To whom correspondence should be addressed.

Unlike most other BK channels (*3*), BK channels (275 ± 9 pS; mean ± SD; $n = 6$) in rat adrenal chromaffin cells undergo rapid inactivation (Fig. 1). The cytoplasmic face of excised, inside-out membrane patches (*9*) containing BK channels was exposed to saline containing a fixed concentration of calcium ($[Ca^{2+}]_i$). We activated BK channels by stepping the patch potential from −40 to +60 mV for 680 ms every 3 s. After opening in the presence of 5 μM $[Ca^{2+}]_i$, BK channels inactivate before the end of the voltage step (Fig. 1A). Single-channel openings were not observed when the patch was bathed in a Ca^{2+}-free solution (Fig. 1B). Ensemble averages generated from idealized single-channel records show that during the voltage step the probability of channels being open (P_O) rises and then decays with a time course reflecting single BK channel activation and subsequent inactivation (Fig. 1C). Consistent with effects of tetraethylammonium (TEA) on other BK channels (*10*), 1 mM TEA applied to an outside-out patch inhibited more than 90% of the single-channel ensemble current (Fig. 1D), whereas 50% inhibition was observed between 200 and

300 μM TEA. When TEA was applied to the cytoplasmic face of inside-out membrane patches, 50% inhibition was observed between 20 and 30 mM. In addition, inactivating BK channels were completely blocked by externally applied 1 mM quinidine, a blocker of BK and other K^+ channels (*11*), but were not affected by external 4-aminopyridine (5 mM), a blocker of A-type K^+ channels (*12*), curare (200 μM), or apamin (200 nM), both of which block voltage-independent, Ca^{2+}-activated K^+ channels (*13*). On the basis of single-channel conductance, the dependence of channel opening on both $[Ca^{2+}]_i$ and voltage, and the differential sensitivity to K^+ channel blockers, these channels appear to belong to the BK ion channel family. However, the rapid and essentially complete inactivation of this channel markedly contrasts with previously described BK channels. Under identical experimental conditions, for example, we have found that BK channels in clonal rat GH_3 pituitary cells exhibit no measurable inactivation, as described by others (n = 12 patches) (*14, 15*).

Next, we wanted to identify factors that influence the rate and extent of BK channel inactivation. This would allow us to determine whether inactivation might be controlled by physiologically relevant parameters and would provide some insight into the mechanism of inactivation so that its properties could be compared to inactivation of purely voltage-gated K^+ channels. To test whether the apparent rate of BK channel inactivation depends on either $[Ca^{2+}]_i$ or membrane depolarization, BK channels were activated either by a voltage step to +60 mV in the presence of different Ca^{2+}_i concentrations (Fig. 2A) or by different depolarizations in the presence of 2 μM $[Ca^{2+}]_i$ (Fig. 2D). Ensemble currents were generated from idealized single-channel records. Currents from Fig. 2, A and D, are shown normalized to peak P_0 with fitted single exponential curves superimposed (Fig. 2, B and E) to emphasize differences among the time constants (τ_i) of current decay. Results from several experiments are summarized in Fig. 2, C and F, where τ_i is plotted as a function of $[Ca^{2+}]_i$ or step potential, respectively. Inactivation was enhanced by increased $[Ca^{2+}]_i$ over the same range of $[Ca^{2+}]_i$ which produced activation (Fig. 2A). Furthermore, at a constant internal Ca^{2+} concentration, the rate of inactivation increased as the test potential was made more positive (Fig. 2B). These data show that the same physiological parameters that activate BK channels also result in inactivation.

A dependence of inactivation rate on $[Ca^{2+}]_i$ and voltage could arise in two ways. First, the microscopic transitions from open to inactivated states could be intrinsically Ca^{2+} and voltage-dependent, or second, an apparent dependence of inactivation rate on Ca^{2+} and voltage could reflect coupling of inactivation to Ca^{2+}- and voltage-dependent steps leading to channel opening. Two observations support the latter possibility. First, with membrane voltage held constant, τ_i saturates as a function of $[Ca^{2+}]_i$ (Fig. 2C), and second, at a constant $[Ca^{2+}]_i$, τ_i tends to saturate as a function of step potential (Fig. 2F). The loss of Ca^{2+} and voltage dependence in τ_i suggests that

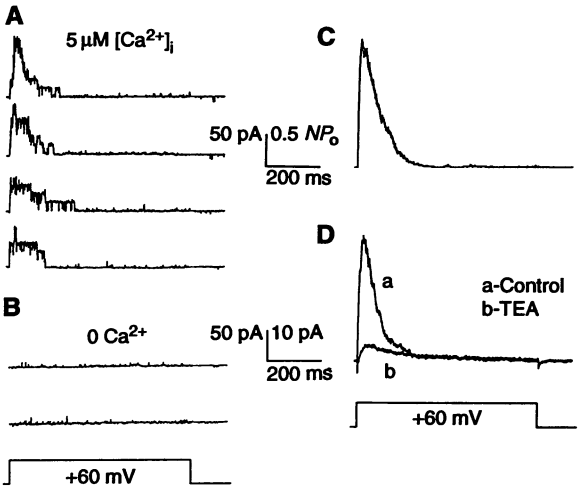

Fig. 1. Inactivating BK channels from rat adrenal chromaffin cells (*26*). (**A**) Consecutive traces from a single membrane patch containing at least eight BK channels are shown. Out of 198 patches, 152 (~77%) contained inactivating BK channels (*27*). (**B**) BK channel openings were not observed when the inside face of the membrane patch was bathed in a solution containing no Ca^{2+} (*28*). The membrane patch and voltage protocol are the same as in (A). Two representative traces are shown. (**C**) Ensemble average BK channels composed of 57 idealized traces recorded from the patch shown in (A). The vertical scale bar (NP_0) represents $N \cdot P_0$, where N = maximum number of channels observed in a patch. (**D**) Blockade of BK current by 1 mM external TEA. Ensemble averages of single BK channels recorded in an outside-out patch perfused with external saline (larger trace) then with external saline plus 1 mM TEA (smaller trace). Washout of TEA with external saline restored BK current to control amplitude. Internal Ca^{2+} = 2 μM, aspartic acid replaced Cl^- as the major anion in this experiment. External saline: 140 mM KCl, 20 mM Hepes, 5 mM EGTA, pCa 7 (pH 7.4 with KOH), 285 to 315 mosM. Internal saline: 140 mM KCl, 20 mM Hepes, 5 mM EGTA (pH 7.0 with KOH), 285 to 315 mosM, pCa as indicated.

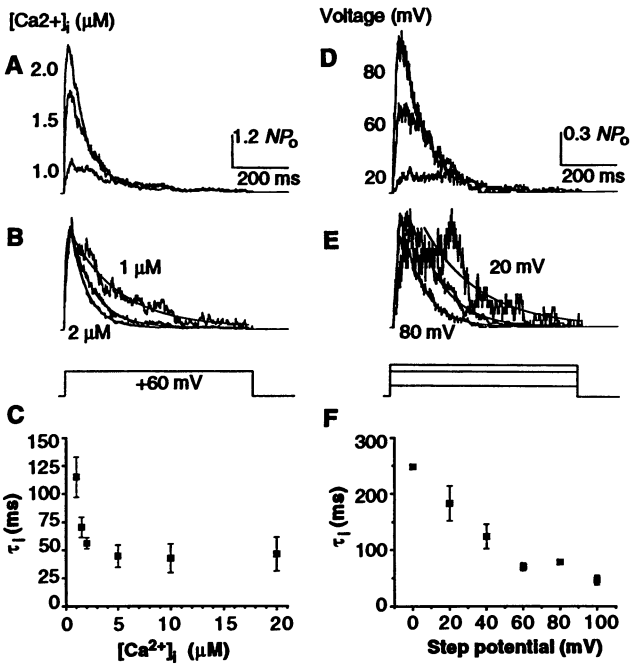

Fig. 2. Ca^{2+} and voltage dependence of apparent inactivation rate. (**A**) Ensemble averages of BK current in a single inside-out patch depolarized from −40 to +60 mV in the presence of 1, 1.5, or 2 μM $[Ca^{2+}]_i$. (**B**) Traces from (A) scaled to peak amplitude and fitted with single exponential functions of the form $A \cdot \exp(-t/\tau_i) + B$. (**C**) Time constant of current decay (τ_i) plotted as a function of $[Ca^{2+}]_i$. Experiments were similar to those in (A). Each point represents the mean ± SEM of three to eight determinations in 13 patches. (**D**) Ensemble averages of BK current in a single inside-out patch depolarized to +20, +60, and +80 mV in the presence of 2 μM $[Ca^{2+}]_i$. (**E**) Traces from (D) scaled to peak amplitude and fitted with single exponential functions as in (B). (**F**) Time constant of current decay (τ_i) plotted as a function of potential. Experiments were similar to those in (E). Each point represents the mean ± SEM of 3 to 11 determinations in 20 patches except the points at 0 and +80 mV, which represent single experiments. Fitting exponential functions to ensemble currents was accomplished with a nonlinear least-squares procedure based on the Levenberg-Marquardt routine (RMSSQ subroutine of the IMSL statistical library, Bellaire, Texas) for minimization of residuals. External saline contained 15.4 mM KCl, 124.6 mM NaCl, 20 mM Hepes, 5 mM EGTA, pCa 7 (pH 7.4 with NaOH). Internal saline as in Fig. 1.

the transitions into inactivated states are themselves Ca^{2+}- and voltage-independent and that τ_i derives its observed Ca^{2+} and voltage dependence from the Ca^{2+} and voltage dependence of activation. That is, as BK channels are activated more rapidly, they inactivate more rapidly, and, when activation is maximal, so is inactivation. Inactivation coupled to voltage-dependent activation has been proposed for many purely voltage-gated channels (*16*). Our results extend this idea by suggesting that the apparent voltage and Ca^{2+} dependence of BK channel inactivation is due to coupling of inactivation to voltage- and Ca^{2+}-dependent activation. Saturation of τ_i with higher $[Ca^{2+}]_i$ also provides evidence against the argument that inactivation may be caused by first-order blockade of the open channel by $[Ca^{2+}]_i$, which predicts a linear rather than asymptotic relation between blocking rate and $[Ca^{2+}]_i$ (*17*).

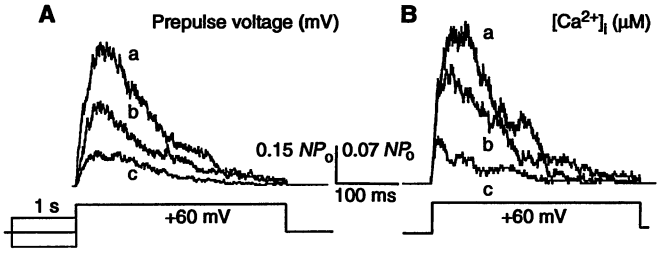

Fig. 3. BK channel availability depends on membrane voltage and $[Ca^{2+}]_i$. (**A**) A depolarizing voltage prepulse increases resting inactivation of BK channels at a fixed $[Ca^{2+}]_i$. Ensemble averages of BK channels in a single inside-out patch show that the amount of BK current activated decreases as membrane potential before the voltage step is made more positive. Similar results were obtained in five patches. Prepulse voltages for a, b, and c were −80 mV, −40 mV, and 0 mV, respectively. (**B**) Elevation of $[Ca^{2+}]_i$ increases resting inactivation of BK channels in patches held at a fixed potential. Ensemble averages of BK channels from the same patch as in (A) show that the amount of BK current decreases with higher $[Ca^{2+}]_i$. Similar results were recorded in six patches. Solutions as in Fig. 2. The $[Ca^{2+}]_i$ for a, b, and c were 5 μM, 10 μM, and 20 μM, respectively.

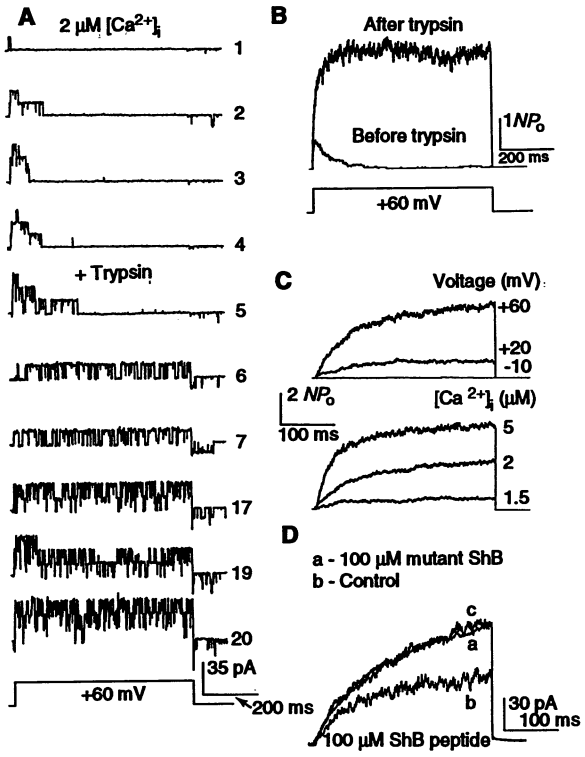

Fig. 4. (**A**) Trypsin removes inactivation from BK channels. BK channels recorded in an inside-out patch depolarized from −40 to +60 mV every 3 s in the presence of 2 μM $[Ca^{2+}]_i$ (traces 1 to 4) and during exposure to 2 μM $[Ca^{2+}]_i$ + trypsin (0.5 mg/ml) (traces 5 to 7, 17 to 20). Consecutive numbers indicate consecutive voltage jumps. Trypsin application began approximately 1 s before trace 5. The increasing number of noninactivating BK channels reflects the progressive removal of inactivation by trypsin (*29*). Because the K^+ equilibrium potential was 0 mV in this experiment, inward channel openings following the step to +60 mV in traces 6 to 20 are observed. (**B**) Ensemble averages of BK channels before and after cytoplasmic trypsin application. Inward channel openings occurring at the end of the voltage step were not included in the ensemble average. Internal and external salines for (A) and (B) as in Fig. 1. (**C**, top) Trypsin-treated BK channels are voltage-dependent. Ensemble BK current from an inside-out patch depolarized to −10, +20, and +60 mV in the presence of 2 μM $[Ca^{2+}]_i$. Note that $N \cdot P_o$ at −10 mV is close to zero. (**C**, bottom) Trypsin-treated BK channels are Ca^{2+}-dependent. Ensemble averages of trypsin-digested BK channels in an inside-out patch depolarized to +60 mV in the presence of 1.5, 2, and 5 μM $[Ca^{2+}]_i$. (**D**) The Shaker B ball peptide (100 μM) selectively blocks rat adrenal chromaffin cell BK channels. Ensemble averages of trypsin-treated BK channels in an inside-out patch exposed to peptide, mutant peptide (L7A,Q15E,Q20E), or no peptide (control). $[Ca^{2+}]_i$ = 2 μM. Similar results were obtained in five patches. Solutions for (C) and (D) as in Fig. 2. Voltage protocols for (C) and (D) are as in (B); however, note shorter time scale in (C) and (D). Trypsin (type IX from porcine pancreas, Sigma, St. Louis, Missouri) removed inactivation from BK channels in 29 of 29 patches.

Because BK channel inactivation depends on the same parameters that produce activation, the amount of resting inactivation should also depend on resting membrane potential and $[Ca^{2+}]_i$. To test this hypothesis, we activated BK channels in inside-out patches by stepping the membrane potential to +60 mV while varying either holding potential or $[Ca^{2+}]_i$. First, $[Ca^{2+}]_i$ was fixed to 5 μM, and the potential before the voltage step was set to −80, −40, or 0 mV. The amount of current activated at +60 mV decreased as holding potential was made more positive (Fig. 3A). Next, the potential before the voltage jump was fixed to −60 mV while the patch was bathed in either 5, 10, or 20 μM $[Ca^{2+}]_i$. The amount of BK current activated at +60 mV decreased with increasing $[Ca^{2+}]_i$ (Fig. 3B). These results indicate that the amount of BK current available for activation by a voltage step is governed by the membrane potential before the step and by $[Ca^{2+}]_i$. When conditions favor steps leading to channel activation, that is, depolarized holding potential and higher $[Ca^{2+}]_i$, the P_o observed during a positive voltage step is relatively low, indicating an increased likelihood of inactivation before the voltage step. Because the chromaffin cell resting membrane potential is probably between −40 and −50 mV (*18*) and submembrane Ca^{2+} concentrations may reach micromolar concentrations (*19*), these results suggest that the amount of BK current available for activation can be actively regulated by normally occurring changes in membrane voltage and submembrane Ca^{2+}.

Intracellular application of the protease trypsin selectively removes inactivation from voltage-gated K^+ channels (6), providing support for the "ball and chain" model of inactivation (*20*) in which a protease-sensitive, cytoplasmic domain of the channel protein binds and occludes the open channel (*7*). We tested whether rat adrenal chromaffin cell BK channels possess a similar mechanism of inactivation by applying trypsin to BK channels in excised, inside-out patches of membrane. A brief application of trypsin rapidly and irreversibly caused BK channels to open in long-lived bursts, consistent with removal of inactivation (Fig. 4A). The amplitude of the ensemble current after trypsin digestion was consistently larger than the peak current before trypsin (Fig. 4B). The large increase in peak current after trypsin reflects a higher maximal number of channels that simultaneously open during a voltage step (three before trypsin, seven after trypsin). A comparison of the average peak P_o

before and after trypsin application (Fig. 4B) suggests that at −40 mV and 2 μM $[Ca^{2+}]_i$ the probability that an inactivating BK channel will open during a depolarizing voltage step is about 25% (*21*). Two factors may contribute to this low probability of opening. (i) BK channels may have access to inactivated states directly from closed states so that during a voltage step channels would not necessarily open before inactivating (*22*). (ii) Because $[Ca^{2+}]_i$ was fixed at 2 μM in this experiment, a high level of resting inactivation may have been established. The effect of trypsin was inhibited both by soybean trypsin inhibitor (0.3 mg/ml) and by leupeptin (100 μM) and was not observed when trypsin was applied to the extracellular face of the membrane. Trypsin removes inactivation from BK channels without grossly altering other properties of the channel. Ensemble averages of trypsin-treated BK channels show a noninactivating current that retains voltage dependence (Fig. 4C, top) and $Ca^{2+}{}_i$ dependence (Fig. 4C, bottom). In addition, the conductance of BK channels was not significantly changed after trypsin digestion (275 ± 9 pS before trypsin; $n = 6$; versus 270 ± 12 pS after trypsin; $n = 6$). Although trypsin is a nonspecific protease that can cleave at many sites on a channel protein, the high degree of specificity with which it removes inactivation supports the notion that it is digesting an exposed protein domain that is distinct from voltage-sensing and $Ca^{2+}{}_i$-binding portions of the channel protein.

Inactivation that involves a cytoplasmic, protease-sensitive protein domain is reminiscent of N-type inactivation described for Shaker BK^+ channels in which the NH_2-terminal 20 amino acids of the channel protein block the open channel to cause inactivation (*7*). Mutant, noninactivating Shaker K^+ channels can be made to inactivate by internal application of a peptide corresponding to the Shaker B (ShB) NH_2-terminus (*7*). This ShB ball peptide is known to block noninactivating BK channels incorporated into lipid bilayers from both rat brain and coronary artery smooth muscle (*23*). Internal application of 100 μM purified ShB peptide blocks trypsin-treated rat chromaffin cell BK channels by about 50% (Fig. 4D) (*24*). Trypsin digestion of the ShB peptide removed its ability to block BK channels ($n = 3$), and application of a ShB peptide with three amino acid substitutions (*25*) did not block the channels appreciably. Blockade by the ShB peptide shows no time dependence, suggesting that the peptide has access to its binding site whether the channel is open or closed. Thus, a potential binding site for an inactivating domain may be available while channels are at rest, consistent with the high level of BK channel resting inactivation we have observed. Although BK channel inactivation may involve the ShB peptide binding site or some other site on the channel protein, our results demonstrate that a binding site for the ShB peptide is conserved in rat chromaffin cell BK channels.

We have shown that rat adrenal chromaffin cells possess a BK channel that undergoes rapid and virtually complete inactivation. Similar to N-type inactivation characterized for Shaker B K^+ channels, BK channel inactivation derives an apparent dependence on conditions which lead to channel opening, but has little intrinsic dependence on these factors. In addition, the availability of BK channels for activation is reduced when submembrane Ca^{2+} is elevated and the plasma membrane is depolarized. BK channel inactivation is removed by trypsin digestion, and the channels specifically bind the ShB inactivating domain, suggesting additional similarity between this BK channel and the ShB channel.

The observation that some Ca^{2+}-activated K^+ channels exhibit rapid inactivation adds a new level of complexity to the role that these channels may play in regulating cellular excitability. Furthermore, our findings indicate that this BK channel uses a mechanism for inactivation analogous to that used by other voltage-gated K^+ channels, demonstrating that structural features found among members of the voltage-gated K^+ channel family may extend to the family of voltage- and Ca^{2+}-activated K^+ channels.

REFERENCES AND NOTES

1. O. H. Peterson and Y. Maruyama, *Nature* **307**, 693 (1984); A. Marty, *Trends Neurosci.* **12**, 420 (1989).
2. B. S. Pallotta, K. L. Magleby, J. N. Barrett, *Nature* **293**, 471 (1981); J. N. Barrett, K. L. Magleby, B. S. Pallotta, *J. Physiol. (London)* **331**, 211 (1982); A. L. Blatz and K. L. Magleby, *Nature* **323**, 718 (1986); R. Latorre, A. Oberhauser, P. Labarca, O. Alvarez, *Annu. Rev. Physiol.* **51**, 385 (1990).
3. Evidence for BK channel inactivation has been described in B. S. Pallotta [*J. Physiol. (London)* **363**, 501 (1985)] and Y. Ikemoto, K. Ono, A. Yoshida, and N. Akaike [*Biophys. J.* **56**, 207 (1989)].
4. A. Marty, *Trends Neurosci.* **6**, 262 (1983); R. Latorre and C. Miller, *J. Membr. Biol.* **71**, 11 (1983).
5. A. B. MacDermott and F. F. Weight, *Nature* **300**, 185 (1982); B. Lancaster and P. Pennefather, *J. Physiol. (London)* **387**, 519 (1987); D. G. Lang and A. K. Ritchie, *ibid.* **425**, 117 (1990).
6. T. Hoshi, W. N. Zagotta, R. W. Aldrich, *Science* **250**, 533 (1990).
7. W. N. Zagotta *et al.*, *ibid.*, p. 568.
8. W. Stühmer *et al.*, *EMBO J.* **8**, 3235 (1989); J. P. Ruppersberg *et al.*, *Nature* **345**, 535 (1990).
9. O. P. Hamill, A. Marty, E. Neher, B. Sakmann, F. J. Sigworth, *Pfluegers Arch.* **393**, 254 (1981).
10. G. Yellen, *J. Gen. Physiol.* **84**, 157 (1984).
11. N. Iwatsuki and O. H. Peterson, *Biochim. Biophys. Acta* **819**, 249 (1985); I. Findlay *et al.*, *FEBS Lett.* **185**, 4 (1985).
12. S. H. Thompson, *J. Physiol. (London)* **265**, 465 (1977).
13. G. Romey and M. Lazdunski, *Biochem. Biophys. Res. Commun.* **118**, 669 (1984); M. Nohmi and K. Kuba, *Brain Res.* **301**, 146 (1984); J. W. Goh and P. S. Pennefather, *J. Physiol. (London)* **394**, 315 (1987).
14. D. G. Lang and A. K. Ritchie, *Pfluegers Arch.* **410**, 614 (1987).
15. Several different cell types were screened for inactivating BK channels, identified in inside-out patches by their large conductance and sensitivity to $[Ca^{2+}]_i$. The results of this survey are expressed as [cell type (number of patches containing inactivating BK channels per total number of patches containing BK channels)]: bovine chromaffin cells (2/4); PC12 cells, nonnerve growth factor (NGF)–differentiated (8/12); rat superior cervical ganglion neurons (0/5); quail fibroblasts (QT-6 clonal cell line) (0/3); rat cerebellar purkinje and granule cells (0/4); and rat hippocampal neurons (0/3).
16. F. Bezanilla and C. M. Armstrong, *J. Gen. Physiol.* **70**, 549 (1977); R. W. Aldrich, D. P. Corey, C. F. Stevens, *Nature* **306**, 436 (1983); T. Gonoi and B. Hille, *J. Gen. Physiol.* **89**, 253 (1987); W. N. Zagotta, T. Hoshi, R. W. Aldrich, *Proc. Natl. Acad. Sci. U.S.A.* **86**, 7243 (1989); W. N. Zagotta and R. W. Aldrich, *J. Gen. Physiol.* **95**, 29 (1990).
17. C. Vergara and R. Latorre, *J. Gen. Physiol.* **82**, 543 (1983); C. Miller, R. Latorre, I. Reisin, *ibid.* **90**, 427 (1987).
18. Y. Kidokoro and A. K. Ritchie, *J. Physiol. (London)* **307**, 199 (1980).
19. F. Sala and A. Hernandez-Cruz, *Biophys. J.* **57**, 313 (1990); G. J. Augustine and E. Neher, *J. Physiol. (London)* **450**, 247 (1992).
20. F. Bezanilla and C. M. Armstrong, *J. Gen. Physiol.* **70**, 567 (1977).
21. Consistent with this result is the observation that in four patches under the same experimental conditions where the maximum number of BK channels open simultaneously was one or two, the fraction of depolarizing voltage steps during which no channels opened ranged from 0.24 to 0.59. The high number of "null" sweeps in these patches is consistent with a high level of resting inactivation.
22. W. N. Zagotta and R. W. Aldrich, *J. Gen. Physiol.* **95**, 29 (1990); T. E. DeCoursey, *ibid.*, p. 617.
23. S. K. Chung, W. N. Zagotta, R. W. Aldrich, I. B. Levitan, *Soc. Neurosci. Abstr.* **17**, 777 (1991); L. Toro, E. Stefani, R. Latorre, *Biophys. J.* **61**, A379 (1992).
24. ShB peptide used in Fig. 4 was purified by the Protein Chemistry Laboratory, Washington University School of Medicine, St. Louis, MO. Pure ShB peptide obtained from the Protein Nucleic Acid Facility at Stanford University produced about 75% blockade at 70 μM, suggesting that the dissociation constant (K_d) may vary among preparations. The ShB peptide appears to have a higher affinity for Shaker K^+ channels than for some mammalian Shaker homologs [J. P. Ruppersberg, R. Frank, O. Pongs, M. Stocker, *Nature* **353**, 657 (1991); (*7*)].
25. The purified mutant peptide contained the following three amino acid substitutions, expressed as [wild-type residue, residue position, mutant residue]: L7A, Q15E, Q20E. This peptide has an approximately tenfold lower affinity for the Shaker B peptide binding site than does the native ShB peptide (R. Murrell-Lagnado, personal communication).
26. Adrenal medullary chromaffin cells from adult male Sprague-Dawley rats were enzymatically dissociated as described in A. Neely and C. J. Lingle [*J. Physiol. (London)* **453**, 97 (1992)]. Cells were used 2 to 14 days after plating.
27. Fifteen of 198 (~8%) rat chromaffin cell membrane patches contained only noninactivating BK channels. The remainder of patches, 31 of 198 (~16%), contained both inactivating and noninactivating BK channels.
28. Free Ca^{2+} concentrations were calculated with the EGTAETC computer program (apparent stability constant for $Ca^{2+} = 10^{6.26}$ at pH 7.0). For free $[Ca^{2+}]$, greater than 2 μM, 5 mM *N*-hydroxyethylethylenediaminetriacetic acid (HEDTA) rather than EGTA was used to buffer Ca^{2+}. Voltage

protocols were generated with the pClamp software package (Axon Instruments, Foster City, CA) running on an IBM AT computer. Single-channel currents were recorded with an Axopatch 1C patch-clamp amplifier (Axon Instruments), digitally sampled at 2500 Hz, low-pass–filtered at 1 kHz (Bessel filter, −3 dB), and written to computer disk. Analysis of single-channel data was accomplished with in-house software. We corrected raw current traces for leakage and capacitative current by subtracting an average of current activated in the absence of intracellular Ca^{2+}. We idealized single-channel events with a half-amplitude threshold detection routine. Solutions were applied locally to a membrane patch with a glass pipette containing seven separate perfusion lines. Flow in each line was driven by gravity and regulated by computer-controlled solenoid valves. Solution exchange time was approximately 100 ms. Experiments were done at 21° to 24°C.

29. As in Fig. 4A, an apparent initial decrease in opening probability was routinely observed after trypsin application. One interpretation of this observation is that the putative BK channel–inactivating gate, once cleaved from the rest of the channel protein by trypsin, has a higher affinity for its binding site than does the attached gate. Thus, for channels that are exposed to trypsin while inactivated, the cleaved inactivating gate will dissociate from its receptor site more slowly, giving rise to a temporary decrease in P_o.

30. We thank A. S. Evers, E. W. McCleskey, J. M. Nerbonne, and J. H. Steinbach for comments on the manuscript, S. Chakraverty for preparation and maintenance of cell cultures, E. McCleskey for providing the EGTAETC program, and W. N. Zagotta, R. Murrell-Lagnado, and R. W. Aldrich for providing ShB and mutant peptides. Supported by a grant-in-aid from the Missouri Affiliate of the American Heart Association.

27 April 1992; accepted 22 July 1992

A Strategy for Delivering Peptides into the Central Nervous System by Sequential Metabolism

Nicholas Bodor,* Laszlo Prokai, Wei-Mei Wu, Hassan Farag, Sastry Jonalagadda, Masanori Kawamura, James Simpkins

Most peptides do not enter the central nervous system because of their hydrophilic character and the presence of peptidolytic enzymes in the lipoidal blood-brain barrier. To achieve brain delivery of a peptide conjugate, an opioid peptide (enkephalin) was placed in a molecular environment that disguises its peptide nature and provides biolabile, lipophilic functions to penetrate the blood-brain barrier by passive transport. The strategy also incorporates a 1,4-dihydrotrigonellinate targetor that undergoes an enzymatically mediated oxidation to a hydrophilic, membrane-impermeable trigonellinate salt. The polar targetor-peptide conjugate that is trapped behind the lipoidal blood-brain barrier is deposited in the central nervous system. Analgesia was observed with "packaged" enkephalin but not with the unmodified peptide or lipophilic peptide precursors.

The blood-brain barrier (BBB) is the major obstacle for the development of centrally active peptides. The capillaries in the brain parenchyma possess high-resistance, tight junctions between the endothelial cells (*1*). The cells also lack pores; thus, the brain capillary endothelium behaves like a continuous lipid bilayer. Diffusion through this layer, the physical BBB, is largely dependent on the lipid solubility of the solute. Water-soluble molecules (for example, glucose, essential amino acids, and glutamate) enter the brain almost exclusively by carrier-mediated transport (*2*). Most peptides, such as the naturally occurring enkephalins, are hydrophilic and do not cross the BBB, because of the absence of specific transport systems in the membrane. Their metabolic instability also implies that the highly active neuropeptide-degrading enzymes (*3*), such as the capillary-bound aminopeptidase (*4*), arylamidase (*5*), and enkephalinase (*6*), constitute an enzymatic BBB for peptides that results in their rapid cleavage.

Various strategies have been applied to direct centrally active peptides into the brain. An invasive procedure that includes surgical implantation of an intraventricular catheter followed by pharmaceutical infusion into the ventricular compartment delivers a metabolically unstable peptide only to the surface of the brain (*7*). Transient opening of the tight junctions by the intracarotid infusion of an osmotically active substance (mannitol, arabinose) in high concentrations (>1 M) may facilitate an indiscriminate delivery of molecules that otherwise cannot cross the BBB (*8*). However, this procedure is accompanied by severe toxic effects, which can lead to inflammation, encephalitis, and seizures. These invasive procedures are only justified for some life-threatening conditions and are not acceptable for less serious illnesses.

A noninvasive method for peptide delivery into the central nervous system (CNS) has been suggested that uses the formation of chimeric peptides (*9*). This strategy relies on the presence of specific receptor-mediated transcytosis systems in the BBB for certain larger peptides such as insulin, insulin-like growth factor, transferrin, and albumin. Covalently coupling (for example, through disulfide bonds) a nontransportable peptide to these transport vectors results in a chimeric peptide that can also undergo receptor-mediated transcytosis, and the active peptide can be released by its enzymatic cleavage in the CNS. However, these carriers are not brain-specific, as uptake by nonneural cells or cells outside the CNS has also been shown (*10*). Low amounts of the peptide relative to the carrier molecule and the receptor-based cellular transport mechanism that has physiologically limited transporter capacity (saturable) also prevent pharmacologically significant amounts from entering the brain. Finally, release of the active peptide from the conjugate has not been documented.

Our approach is an enzyme-based strategy and is distinct from a simple pharmacologically based approach in which peptide "prodrugs" are applied that are lipophilic esters or amides of the molecule (*11*). Although the acquired lipophilicity of these prodrugs may assure penetration to the BBB (and to other membranes), this is not the sole factor involved in the transport of a peptide into the CNS. BBB transport of cyclosporin, which is one of the most lipid-soluble peptides, is paradoxically low as a result of peptide degradation (*12*). The enzymatic BBB is also circumvented by our approach. The prototype of the system (Fig. 1) has been designed and evaluated for the enkephalin analogs, (D-Ala^2)-Leu-enkephalin and (D-Ala^2)-(D-Leu^5)-enkephalin. Both the COOH-terminus and the NH_2- terminus of the molecule have been modified in such a way as to increase the lipid solubility of the peptide and also to prevent cleavage by the BBB aminopeptidases. Additionally, the 1,4-dihydrotrigonellinate redox targetor (T) exploits the unique architecture of the BBB, which allows for the influx of the lipid soluble neutral form, but it is not permeable to the positively charged form. The redox targetor has proved to be widely applicable for brain targeting of a variety of substances (*13*), and its attachment alone results in brain-specific delivery for small molecules such as dopamine (*14*).

The enkephalins are sensitive to cleavage by endopeptidases at the Gly^3-Phe^4 peptide bond. Cholesteryl, a bulky and lipophilic steroidal moiety (L), provides an ester function that increases the lipid solubility and also hinders the COOH-terminal portion of the peptide from being recognized by peptide-degrading enzymes.

Center for Drug Discovery, College of Pharmacy, J. Hillis Miller Health Center, University of Florida, Gainesville, FL 32610.

*To whom correspondence should be addressed.